Approximate spring balancing of linkages to reduce actuator requirements

ARTICLE *in* MECHANISM AND MACHINE THEORY · APRIL 2015

Impact Factor: 1.66 · DOI: 10.1016/j.mechmachtheory.2014.11.014

2 AUTHORS:

Sushant Veer
University of Delaware

Sujatha Srinivasan
Indian Institute of Technology Madras

Approximate Spring Balancing of Linkages to Reduce Actuator Requirements

Sushant Veer[a], S. Sujatha[b,*]

[a]Department of Mechanical Engineering, University of Delaware, Newark, DE 19716, USA
[b]Department of Mechanical Engineering, Indian Institute of Technology Madras, Chennai 600036, India

Abstract

The potential benefit of applying gravity balancing to orthotic, prosthetic and other wearable devices is well recognized, but practical applications have been elusive. Although existing methods provide exact gravity balance, they require additional masses or auxiliary links, or all the springs used originate from the ground, which makes the resulting device bulky and space-inefficient. This work presents a new method that is more practical than existing methods to provide approximate gravity balancing of mechanisms to reduce actuator loads. Current balancing methods use zero-free-length springs or simulate them to achieve balancing. Here, non-zero-free-length springs can be used directly. This new method allows springs to be attached to the preceding parent link, which makes the implementation of spring balancing practical. The method is applicable to planar and spatial, open and closed kinematic chains. Applications of this method to a lower-limb orthosis and a manually-operated sit-to-stand wheelchair mechanism are presented. Results show considerable reduction in actuator requirements with practical spring design and arrangements.

Keywords: Spring balancing, Approximate balancing, Orthosis, Prosthesis, Exoskeleton, Sit-to-stand wheelchair

*Corresponding Author, Tel: +91-44-2257-4728, Fax: +91-44-2257-4652
Email addresses: veer@udel.edu (Sushant Veer), sujsree@iitm.ac.in (S. Sujatha)

1. Introduction

To considerably reduce the actuator requirements, gravity balancing has been used in anthropomorphic robots and other linkages that have to work against gravity. As the need for gravity balancing is well recognized, there are many techniques available. Exact (or perfect) static balancing of links can be obtained by adding counterweights, but this leads to an overall increase in inertial mass which is undesirable, especially if the application is to wearable devices such as orthoses, prostheses and exoskeletons. Static balancing using springs is more suitable for such applications since springs provide greater flexibility in attachment points.

Rahman et al.[1] present techniques for balancing a single link perfectly using zero-free-length springs and extend it to balancing an n-link open chain with the help of auxiliary links. Although the use of auxiliary links provides perfect balancing, the additional links occupy a lot of space and increase the mass and bulkiness of the mechanism. In addition, these techniques assume zero-free-length springs, which further contributes to the complexity of the design. Similarly, Streit and Shin[2] use zero-free-length springs for spring balancing of closed loop linkages. Agrawal and Agrawal [3] provide an approximate static balancing method using non-zero-free length springs but with the need for auxiliary links. Gopalswamy et al.[4] present an approximate static balancing technique for a parallelogram linkage using torsional springs. Carwardine[5] and Riele and Herder[6] present perfect balancing techniques using non-zero-free-length springs but their solutions have specific geometric configurations that may not be usable in every situation due to space and size limitations.

This work was inspired by the recent method devised by Deepak and Ananthasuresh [7] which provides for perfect gravity balancing using only springs and no auxiliary links. However, their method again requires zero-free-length springs or the simulation thereof using non-zero-free-length springs. In addition, all the springs in their technique have one end pivoted to the ground. These conditions pose considerable problems in many situations like wearable devices where cosmetic appearance and available space are major constraints.

There have been other techniques for approximate spring balancing and for determining optimal spring pivot locations. Segla[8] presents an optimization using genetic algorithm for a six-DOF robot mechanism with the gripper force as the objective function. Huang and Roth[9, 10] use the principle of virtual work for placement of springs at apt positions. Mahalingam and Sharan[11] present an optimization for optimal location of spring pivots and relevant spring characteristics to reduce the unbalanced moment. Idlani et al.[12] present a technique with specified potential energy at precision points. Brinkman and Herder[13] present a technique for optimal spring balanced mechanisms by a method they call field fitting in which the energy field of the gravity balancer is matched as closely as possible to the energy field required for a balanced system. Here, we propose an optimization-based approximate spring balancing technique that helps predict the relevant spring parameters and spring pivot locations as well. The technique is presented in a generic fashion, which would allow it to be implemented in a variety of mechanisms.

This work is motivated by the need for practical implementation of balancing in mechanisms that have stringent space and mass constraints, like orthoses, prostheses and exoskeletons. Previous attempts at using gravity balancing for such devices have resulted in complex and bulky mechanisms[14, 15, 16]. Ciupitu et al.[17] propose some mechanisms in their work that have medical relevance, but all these mechanisms have springs attached to the ceiling, greatly hindering the mobility and increasing the space requirements.

The method used in this work, apart from being space efficient, makes design easier by eliminating the step that involves simulating zero-free-length springs with non-zero-free-length springs. Springs with non-zero-free-lengths can be directly used. The method is very general and can be applied to open and closed loop kinematic chains comprising planar or spatial mechanisms. We demonstrate the design of the springs for reducing actuation requirements for a lower-limb orthosis (open-loop) and a manually operated sit-to-stand wheelchair mechanism (closed-loop).

To overcome the requirement of locating one pivot of each spring on the fixed link [7], we investigated using child-parent connections to balance a serial chain of links. We show in the following section that exact balancing is not possible with this configuration, even with zero-free-length springs.

The paper is organized as follows: the next section proves that perfect spring balancing is not possible by child-parent spring connections for a two-link serial manipulator. Section 3 describes the problem formulation for approximate spring balancing of open-link planar chains, a four-bar linkage and open-link spatial chains. Section 4 presents examples - the method is applied to design gravity balancing of a two-link lower-limb orthosis, and to reduce the actuator requirement of a manually operated sit-to-stand wheelchair mechanism. Section 5 presents conclusions of the present work. Section 6 presents the nomenclature used.

2. Proof to show that perfect spring balancing is not possible by child-parent spring connections

We take the simple case of a two-link open kinematic chain connected by revolute joints as shown in Figure 1. The notation used is as indicated in Section 6. Zero-free-length springs are assumed in this section, for the sake of

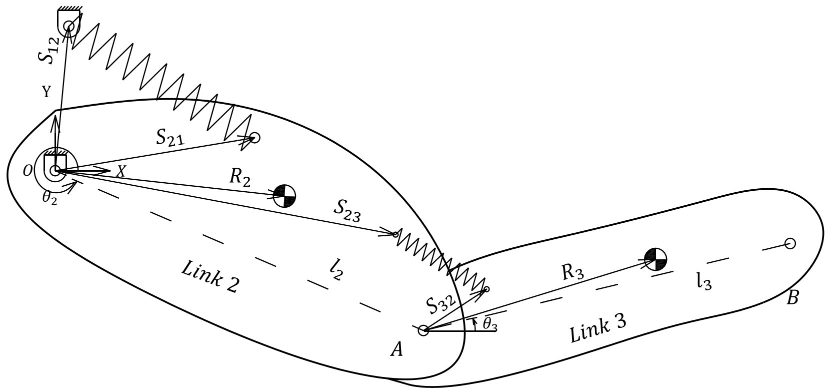

Figure 1: Two-link open kinematic chain

simplifying the proof. The total potential energy of the system is given by

$$\begin{aligned} PE =& m_2 g r_2 \sin(\theta_2 + \alpha_2) + m_3 g [r_3 \sin(\theta_3 + \alpha_3) + l_2 \sin\theta_2] \\ &+ \frac{1}{2} K_1 (\|\mathbf{S}_{21} - \mathbf{S}_{12}\|^2) + \frac{1}{2} K_2 (\|\mathbf{S}_{23} - \mathbf{S}_{32} - \mathbf{L}_2\|^2). \end{aligned} \tag{1}$$

Expanding and simplifying, we get

$$\begin{aligned} PE =& m_2 g r_2 \sin(\theta_2 + \alpha_2) + m_3 g [r_3 \sin(\theta_3 + \alpha_3) + l_2 \sin\theta_2] \\ &+ \frac{1}{2} K_1 [\|\mathbf{S}_{12}\| + \|\mathbf{S}_{21}\|^2 \\ &\qquad - 2 \|\mathbf{S}_{12}\| \|\mathbf{S}_{21}\| \cos(\theta_2 + \beta_{21} - \beta_{12})] \\ &+ \frac{1}{2} K_2 [\|\mathbf{S}_{23}\| + l_2^2 + \|\mathbf{S}_{32}\|^2 \\ &\qquad + 2 l_2 \|\mathbf{S}_{32}\| \cos(\theta_3 - \theta_2 + \beta_{32}) \\ &\qquad - 2 l_2 \|\mathbf{S}_{23}\| \cos\beta_{23} \\ &\qquad - 2 \|\mathbf{S}_{32}\| \|\mathbf{S}_{23}\| \cos(\theta_3 - \theta_2 + \beta_{32} - \beta_{23})]. \end{aligned} \tag{2}$$

The potential energy is only a function of θ_2 and θ_3 as all the other quantities are constants. If spring balancing has to be exact, then,

$$\nabla(PE) = \begin{bmatrix} \dfrac{\partial(PE)}{\partial\theta_2} \\ \dfrac{\partial(PE)}{\partial\theta_3} \end{bmatrix} = \begin{bmatrix} 0 \\ 0 \end{bmatrix} \tag{3}$$

for all θ_2 and θ_3. This implies that

$$\begin{aligned} \frac{\partial(PE)}{\partial\theta_2} =& m_2 g r_2 \cos(\theta_2+\alpha_2) + m_3 g l_2 \cos\theta_2 \\ &+ K_1 \|\mathbf{S}_{12}\| \|\mathbf{S}_{21}\| \sin(\theta_2+\beta_{21}-\beta_{12}) \\ &+ K_2 l_2 \|\mathbf{S}_{32}\| \sin(\theta_3-\theta_2+\beta_{32}) \\ &- K_2 \|\mathbf{S}_{32}\| \|\mathbf{S}_{23}\| \sin(\theta_3-\theta_2+\beta_{32}-\beta_{23}) = 0, \end{aligned} \tag{4}$$

and

$$\begin{aligned} \frac{\partial(PE)}{\partial\theta_3} =& m_3 g r_3 \cos(\theta_3+\alpha_3) \\ &- K_2 l_2 \|\mathbf{S}_{32}\| \sin(\theta_3-\theta_2+\beta_{32}) \\ &+ K_2 \|\mathbf{S}_{32}\| \|\mathbf{S}_{23}\| \sin(\theta_3-\theta_2+\beta_{32}-\beta_{23}) = 0, \end{aligned} \tag{5}$$

Solving these two equations for K_1 and K_2, we get,

$$K_1 = \frac{-[m_2 g r_2 \cos(\theta_2+\alpha_2) + m_3 g l_2 \cos\theta_2 + m_3 g r_3 \cos(\theta_3+\alpha_3)]}{\|S_{12}\| \|S_{21}\| \sin(\theta_2+\beta_{21}-\beta_{12})}. \tag{6}$$

$$K_2 = \frac{m_3 g r_3 \cos(\theta_3+\alpha_3)}{l_2 \|\mathbf{S}_{32}\| \sin(\theta_3-\theta_2+\beta_{32}) - \|\mathbf{S}_{32}\| \|\mathbf{S}_{23}\| \sin(\theta_3-\theta_2+\beta_{32}-\beta_{23})}. \tag{7}$$

Let

$$C_1 = \frac{\cos(\theta_2+\alpha_2)}{\sin(\theta_2+\beta_{21}-\beta_{12})}, \tag{8}$$

$$C_2 = \frac{\cos\theta_2}{\sin(\theta_2+\beta_{21}-\beta_{12})}, \tag{9}$$

and

$$C_3 = \frac{\cos(\theta_3+\alpha_3)}{\sin(\theta_2+\beta_{21}-\beta_{12})}. \tag{10}$$

Assume the case in which θ_2 is kept constant but θ_3 is varied. Since C_1 and C_2 depend only on θ_2, they remain constant, but C_3 varies; therefore, K_1 varies as is evident in (6). Hence, K_1 is not constant for all $\{\theta_{2,}\theta_3\}$ in configuration space where θ_2 and θ_3 are independent of each other.

The basis set of this configuration space is $\{\theta_2, \theta_3\}$. The basis can also be taken as $\{\theta_3 - \theta_2, \theta_3\}$ since these two quantities are also linearly independent and the dimension of the configuration space remains the same. If we keep $(\theta_3 - \theta_2)$ constant and vary only θ_3, the denominator of (7) remains constant, but the numerator varies. Hence, K_2 cannot remain constant over the entire workspace.

This proves that exact gravity compensation with springs of invariant spring constants is impossible over an entire configuration space using serial child-parent connections. To the best of the authors' knowledge, this proof has not been presented before in the literature.

3. Methodology

Perfect balancing implies that the potential energy of the system is made invariant over the configuration space. This result is shown easily by expressing the dynamics of a mechanism using the Lagrangian formulation [18, pp 135]. Let q be the vector of the generalized coordinates of the mechanism and τ be the vector of all the generalized forces. Then, the dynamics can be expressed as

$$\frac{d}{dt}\frac{\partial(KE)}{\partial \dot{q}} - \frac{\partial(KE)}{\partial q} + \frac{\partial(PE)}{\partial q} = \tau. \tag{11}$$

For static balancing, $KE = 0$ in (11), reducing the expression of torque to $\tau = \nabla(PE)$ where the gradient operator is with respect to the configuration variables.

By using a spring for static balancing, the net potential energy of the system is made to remain constant, i.e. $\nabla(PE) = 0$, for the entire configuration space.

The spring stores energy when gravitational potential energy reduces, and it releases energy when gravitational potential energy of the system increases. If perfect spring balancing is not possible, approximate spring balancing can be achieved by minimizing the variance of potential energy over the configuration space. This is the central theme of this work.

3.1. General Formulation of the Optimization

Let $\mathbf{x}$ be the vector representing the configuration space variables and $\mathbf{y}$ be all the design parameters that can be altered such as the spring free length, locations of attachment points of the spring, etc. K_i represents the spring constant of the spring connecting the i$^{th}+1$ child link to its parent, the ith link. The fixed link is the first link. Then,

$$PE = f(\mathbf{x}, \mathbf{y}, K_1, K_2, ..., K_n). \tag{12}$$

For each set of $A = (\mathbf{y}, K_1, K_2, ..., K_n)$, the PE at every $\mathbf{x}$ in space is found. Note that A cannot include kinematic parameters like link lengths, position of center of mass etc. as that would imply altering the mechanism. The goal of this work is to find feasible spring design for a mechanism without altering the mechanism itself.

Let the set of all the PE for a particular A be PE_A. The optimization is set up as follows.

$$\begin{aligned} \text{Objective Function :} &\quad variance(PE_A) \\ \text{Control Variable :} &\quad A \\ \text{Compulsory Constraint :} &\quad K_i \geq 0 \text{ for all } i = 1, ..., n \end{aligned} \tag{13}$$

Variance stands for the statistical parameter defined as

$$Variance\,(\sigma^2) \;=\; \frac{\sum_{i=1}^{i=n}(x_i - \bar{x})^2}{n-1}, \tag{14}$$

where $\bar{x}$ is the average of n data points and x_i is the ith data point. These n data points are nodes of a mesh placed on the configuration space. As is expected, with increasing n, the accuracy of the optimal solution increases, but so does the computational effort. An appropriate mesh density can be picked by manually tuning it. An initial coarse mesh is placed on the configuration space which is made finer till the optimal solutions starting from the same initial conditions for different mesh sizes converge.

Apart from the compulsory constraint on K_i, other constraints based on the specific design case can be incorporated.

3.2. Formulation of potential energy variance minimization for open link chains

The method is applied to open-link kinematic chains starting with the classic case of balancing of a single link.

3.2.1. Single link with zero-free-length springs

The configuration for this case is similar to the single link balancing in [1] (see Figure 2).

Using the notation developed in Section 6, the PE in terms of θ_2 is expressed as

$$PE = m_2 g r_2 \sin(\theta_2 + \alpha_2) + \frac{1}{2}K_1(\|\mathbf{S}_{21} - \mathbf{S}_{12}\|^2). \tag{15}$$

The parameter values, $\beta_{12} = 90^o$, $\beta_{21} = 0^o$and $\alpha_2 = 0^o$ chosen to match the configuration provided in [1]. $m_2 = 1$kg, $r_2 = 0.25$m, $\|\mathbf{S}_{12}\| = 0.1$m and $\|\mathbf{S}_{21}\| = 0.2$m were chosen randomly.

An optimization problem was formulated according to (13) with the PE given by (15) and K_1 as the only control variable. The optimization was performed using MATLAB®'s optimization toolbox *fmincon* (gradient based). The result of the optimization gave

$$K_1 = 122.5012\,\text{N/m by PE variance minimization.}$$

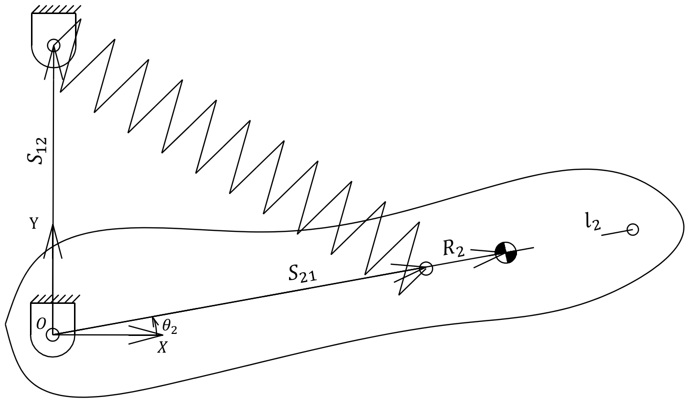

Figure 2: Balancing a single link (adapted from [1])

According to [1], for perfect spring balancing,

$$K_1 = \frac{m_2 g r_2}{\|\mathbf{S}_{12}\| \, \|\mathbf{S}_{21}\|} = 122.5 \text{ N/m}.$$

Thus, the spring constant obtained by optimization closely matches with the exact solution for the single-link case.

3.2.2. Single link with non-zero-free-length springs

For this case, we introduce a non-zero-free-length spring with free length len in place of the zero-free-length-spring in Figure 2. Previous work [1] has shown that exact balancing is not possible with a non-zero-free-length spring connected in the manner shown in Figure 2. The potential energy can be expressed as

$$PE = m_2 g r_2 \sin(\theta_2 + \alpha_2) + \frac{1}{2} K_1 (\|\mathbf{S}_{21} - \mathbf{S}_{12}\| - len)^2. \tag{16}$$

According to the general formulation in Section 3.1, $x = \theta_2$; $A = \begin{bmatrix} len \\ K_1 \end{bmatrix}$.

Apart from the compulsory constraint on K_1 (Section 3.1), another arbitrary constraint is introduced: $len \geq 0.05$m, that is, the free length of the spring should be greater than or equal to 5 cm. Performing the optimization, we get

$$A = \begin{bmatrix} 0.05 \text{ m} \\ 161.39 \text{ N/m} \end{bmatrix}.$$

The spring balancing thus obtained is not exact, but reduces the torque requirement of the system considerably. Figure 3 shows the potential energy distribution over the configuration space for the unbalanced, perfectly balanced and approximately balanced link. Table 1 shows the peak actuator requirements before and after approximate balancing. Figure 4 gives a comparison of the actuation torque values before and after balancing. Note that the torque requirement would be zero for perfect balancing.

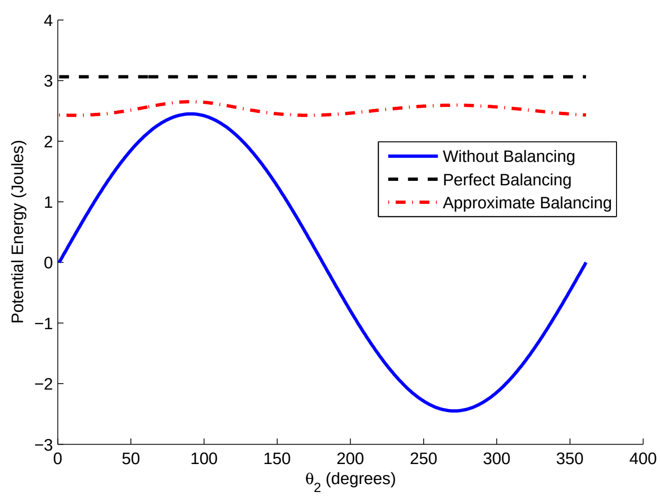

Figure 3: Potential Energy distribution over space(θ_2) for a single link

Table 1: Peak actuator torque for single link with and without approximate balancing

Actuator	Unbalanced peak torque (Nm)	Balanced peak torque (Nm)	Torque reduction
1	2.45	0.23	90.5%

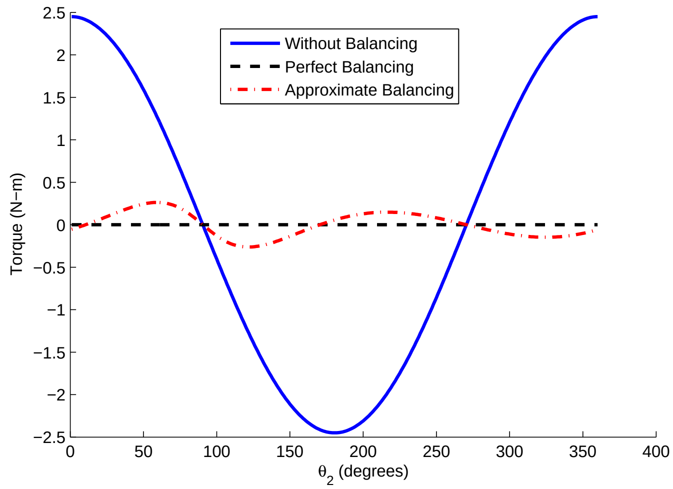

Figure 4: Actuator torque requirement for an unbalanced, perfectly-balanced and approximately-balanced single link

3.2.3. Incorporating additional design parameters for optimization

Throughout this work, for the sake of simplicity, only the spring constants and free length of the springs were used as control variables, with the other parameters kept constant. However, the method for approximate balancing described earlier is very flexible. For example, the position of the spring pivots, $\mathbf{S}_{ij}$ can be included in the control variables so that,

$$A = \begin{bmatrix} \|\mathbf{S}_{ij}\| \\ \beta_{ij} \\ len \\ K \end{bmatrix}.$$

To illustrate, the example in Section 3.2.2 is extended to include more design parameters. The control variables now include the position of the spring pivot, and therefore, $A = \begin{bmatrix} \|\mathbf{S}_{21}\| \\ len_1 \\ K_1 \end{bmatrix}$. In addition to the earlier contraints, a new constraint is added to keep the pivot point of the spring on the link within some desired range, say,

$$0.05 \text{ m} \leq \|\mathbf{S}_{21}\| \leq 0.5 \text{ m}.$$

Potential energy variance minimization yields

$$A = \begin{bmatrix} 0.294 \text{ m} \\ 0.05 \text{ m} \\ 99.96 \text{ N/m} \end{bmatrix}.$$

The optimization using these values yields a peak torque for the actuator of 0.10 Nm which is lower than the earlier value of 0.23 Nm (see Figure 5 and Table 1). This is as expected since more parameters are included as control

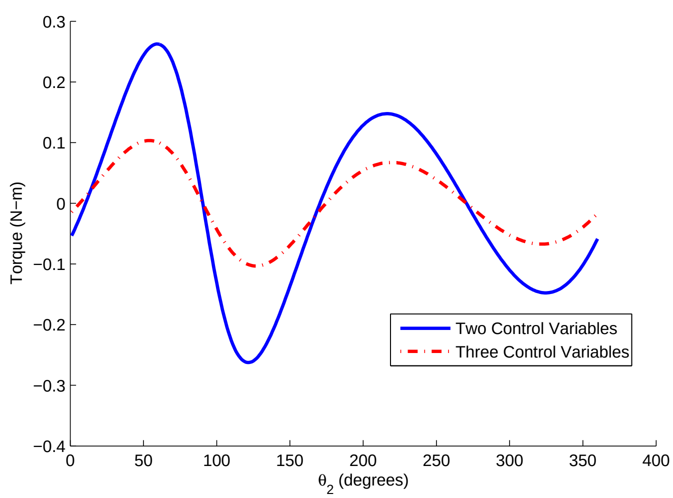

Figure 5: Torque plot with extra design variable for the case in Section 3.2.2

variables in the optimization problem. However, the optimization problem can become very complex when more control variables and constraints are involved. Normal gradient-based methods will lead to local convergence. Heuristic optimization methods may be more appropriate in this scenario for greater likelihood of global convergence.

3.2.4. Generalized formulation for a planar n-link open kinematic chain

The formulation of potential energy variance minimization can be extended to the case of an open kinematic chain with n links (excluding ground) connected by revolute joints. Figure 6 shows an open kinematic chain with n links. The general nomenclature as defined in Section 6 is followed. The basis of the configuration space has n elements $\{\theta_2, \theta_3, ..., \theta_{n+1}\}$ corresponding to the n degrees of freedom.

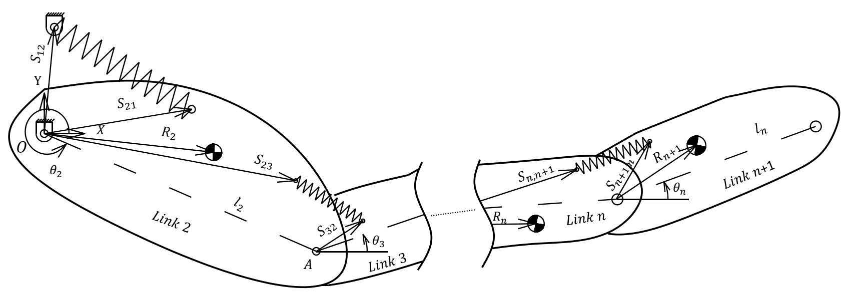

Figure 6: An n-link (excluding ground) open kinematic chain

Each degree of freedom is controlled by an actuator. Let actuator (j) control θ_{j+1}. To reduce the actuator requirement for actuator j, the potential energy variance must be minimized for all the links ahead of it, that is, for links $(j+1)$ to n. Define $\mathbf{L}_i$ as the position vector from joint $i-1$ to i and let $\mathbf{L}_1$ be the zero vector. Then,the potential energy to be used for actuator j is represented by

$$PE^j = \sum_{i=j+1}^{i=n+1} [m_i g r_i^z + \frac{1}{2} K_{i-1}(\|\mathbf{S}_{i,i-1} - \mathbf{S}_{i-1,i} + \mathbf{L}_{i-1}\| - len_{i-1})^2], \qquad (17)$$

$$r_2^z = r_2 \sin(\theta_2 + \alpha_2), \tag{18}$$

$$r_i^z = r_i \sin(\theta_i + \alpha_i) + \sum_{k=2}^{k=i-1} l_k \sin(\theta_k + \alpha_k), \qquad \forall i > 2. \tag{19}$$

Variance($PE^j_{A_j}$) is minimized starting from the distal part of the linkage, that is, from actuator n. The optimization yields A_n. We then optimize for actuator $(n-1)$ using A_n to get A_{n-1}. The process is repeated until A_1 is obtained. Following this sequential procedure breaks down a large nonlinear optimization problem into smaller ones which are more tractable. The intuition behind such a procedure lies in the fact that for serial chain manipulators, an actuator only perceives the load applied further down the chain, thus, springs, links or loads further up the chain would not affect the required torque of the succeeding actuators.

3.3. Formulation of potential energy variance minimization for a planar fourbar linkage

The most common example of a closed-loop kinematic chain is a four-bar linkage. In this section, the method of PE variance minimization is applied to a four-bar linkage, which has four links including the ground. The nomenclature used is the same as that for an n-link open chain. Here, the number of links excluding ground is 3. This optimization technique will work for any number of springs connected between any two bodies. For the sake of simplicity, two springs are considered - one each between the non-floating links and the ground, as shown in Figure 7.

Since a fourbar is a one-degree-of-freedom (DOF) mechanism, the basis set has only one element. Let it be $\{\theta_2\}$. Position analysis of the fourbar is performed first to express θ_3 and θ_4 in terms of θ_2. The PE of the system is given

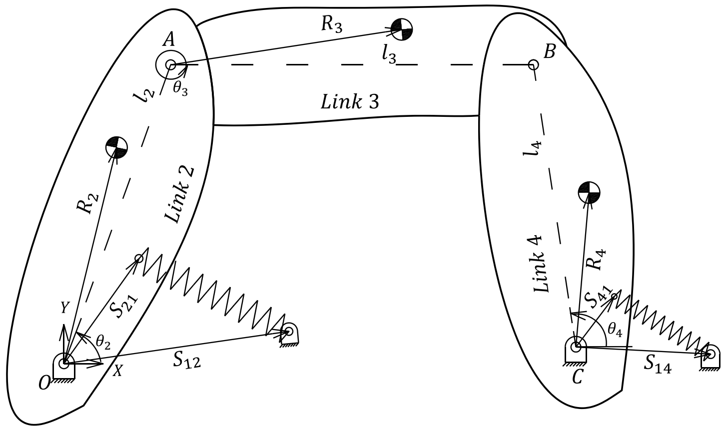

Figure 7: Balancing a general four-bar linkage

by

$$\begin{aligned} PE &= m_2 g r_2 \sin(\theta_2+\alpha_2) + m_3 g(l_2 \sin\theta_2 + r_3\sin(\theta_3+\alpha_3)) \\ &\quad + m_4 g(l_1\sin\theta_1 + r_4\sin(\theta_4+\alpha_4)) + \frac{1}{2}K_1(\|\mathbf{S}_{12}-\mathbf{S}_{21}\| - len_1)^2 \\ &\quad + \frac{1}{2}K_2(\|\mathbf{S}_{14}-\mathbf{S}_{41}\| - len_2)^2. \end{aligned} \tag{20}$$

Potential energy variance minimization is set up as outlined in Section 3.1. In the 1-DOF fourbar with θ_2 as input, K_1 and K_2 can be found simultaneously as only θ_2 is controlled by an actuator.

3.4. Formulation of potential energy variance minimization for an open chain spatial linkage

The spring balancing technique proposed in this work has been applied to the balancing of spatial open chain mechanisms as well. The formulation of the optimization problem remains similar to that for planar mechanisms. Denavit-Hartenberg (D-H) parameters are used to compute the kinematics of a generalized serial n-link spatial mechanism (see figure 8). Coordinate systems o_0 and o_1 are both fixed and do not move. Z_1 is aligned according to the axis of the rotary actuator 1, which may not be in the vertical direction always. The height of the centre of mass of each link is required to calculate the potential energy, hence, the coordinate system 0 with a vertical Z_0 axis is introduced to take care of it. As before, the total potential energy of the links for the entire workspace

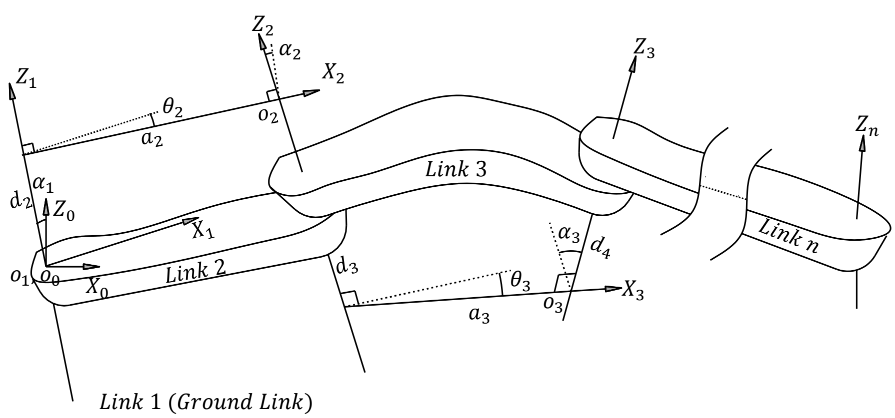

Figure 8: D-H parameter convention(adapted from [19])

is written and the variance minimized to obtain the spring parameters.

In this section any vector V is written in the homogeneous form, i.e.,

$$V = \begin{bmatrix} x \\ y \\ z \\ 1 \end{bmatrix}. \tag{21}$$

From [19], the transformation matrix from i^{th} coordinate system to $(i-1)^{th}$

$\forall i \geq 2$ is given by

$$T_i^{i-1} = \begin{bmatrix} \cos(\theta_i) & -\sin(\theta_i)\cos(\alpha_i) & \sin(\theta_i)\sin(\alpha_i) & a_i\cos(\theta_i) \\ \sin(\theta_i) & \cos(\theta_i)\cos(\alpha_i) & -\cos(\theta_i)\sin(\alpha_i) & a_i\sin(\theta_i) \\ 0 & \sin(\alpha_i) & \cos(\alpha_i) & d_i \\ 0 & 0 & 0 & 1 \end{bmatrix}. \quad (22)$$

Here, angle α_i is the angle between the axis Z_i and Z_{i-1} measured in a plane normal to x_i. a_i is the shortest distance between the axes Z_i and Z_{i-1}. d is the perpendicular distance from the the origin o_{i-1} to the intersection of X_i with Z_{i-1} measured along Z_{i-1} and finally θ_i is the angle between X_{i-1} and X_i measured in a plane normal to Z_{i-1}. Figure 8 represents these symbols on an open chain n-link spatial mechanism.

0^{th} coordinate system is the fixed frame of reference, whereas all others are moving coordinate systems. Note that the 0^{th} coordinate system is not a part of the D-H chain. So the X_1, Y_1 axes orientation for frame 1 can be picked anywhere in the $X_1 - Y_1$ plane after placing Z_1 along the pivot axis, as it is the first frame in the D-H chain.

$$T_1^0 = \begin{bmatrix} \cos(\alpha_i) & 0 & \sin(\alpha_i) & 0 \\ 0 & 1 & 0 & 0 \\ -\sin(\alpha_i) & 0 & \cos(\alpha_i) & 0 \\ 0 & 0 & 0 & 1 \end{bmatrix}, \quad (23)$$

aligns the Z_1 axis with the Z_0 axes. Overlapping the other two axes is not important as for potential energy, only the z component is pertinent. The potential energy of the j^{th} link can be written as

$$PE^j = \sum_{i=j+1}^{i=n+1} \left[m_i g r_i^z + \frac{1}{2} K_{i-1} (\left\| T_i^{i-1} \mathbf{S}_{i,i-1} - \mathbf{S}_{i-1,i} \right\| - len_{i-1})^2 \right]. \quad (24)$$

In the planar case $\mathbf{S}_{i,j}$ and $\mathbf{R}_i$ were expressed in the ground frame but in spatial it is expressed in the i^{th} frame. r_i^z can be obtained by converting the relative centre of mass of the link with respect to the frame Z_0

$$\mathbf{R}_i^0 = T_i^0 \mathbf{R}_i^i, \tag{25}$$

where

$$T_i^0 = T_1^0 T_2^1 T_3^2 ......T_i^{i-1}. \tag{26}$$

The z-component of the position of centre of mass is in the 3^{rd} row of the column vector $\mathbf{R}_i^0$,

$$r_i^z = \mathbf{R}_i^0(3,1). \tag{27}$$

Variance($PE_{A_j}^j$) is minimized starting from the distal part of the linkage, that is, from actuator n. The optimization yields A_n. We then optimize for actuator $(n-1)$ using A_n to get A_{n-1}. The process is repeated until A_1 is obtained.

3.4.1. Spatial single-link balancing

Consider a single link pivoted with its pivot axis making an angle α_1 with the vertical axis. The relevant parameters of the link were taken as:

$$m_2 = 2\text{kg},\ a_2 = 0.3\text{m},\ d_2 = 0\text{m},\ \alpha_1 = 30^o,\ \alpha_2 = 0^o$$

$$\mathbf{R}_2 = \begin{bmatrix} -0.1\text{m} \\ 0 \\ 0 \\ 1 \end{bmatrix}, \mathbf{S}_{12} = \begin{bmatrix} 0 \\ 0 \\ 0.05\text{m} \\ 1 \end{bmatrix}, \mathbf{S}_{21} = \begin{bmatrix} -0.2\text{m} \\ 0 \\ 0 \\ 1 \end{bmatrix}$$

Here $\mathbf{S}_{21}$ and $\mathbf{R}_2$ are written with respect to the moving coordinate system 2 on the link (refer Figure 8).

Potential energy variance minimization was performed with these parameters. Figure 9 shows the potential energy distribution at $\alpha_1 = 30^o$. The K obtained was 784 N/m. An interesting result to note here is that when varying α_1 alone while keeping the other parameters constant, the spring constant obtained is constant for perfect balancing, except for the case of $\alpha_1 = 0$. For $\alpha_1 = 0$

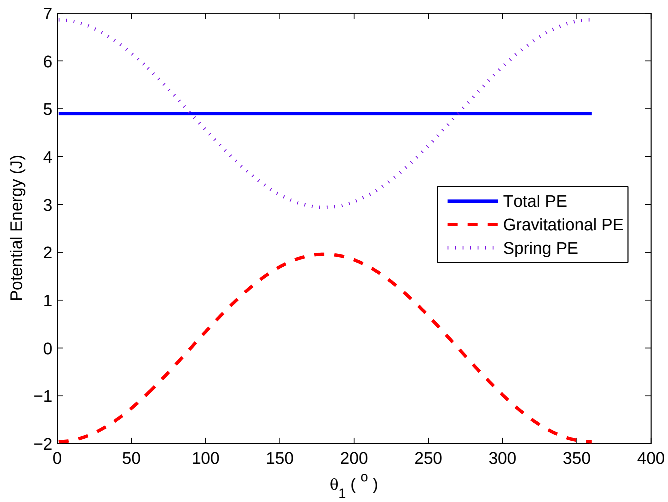

Figure 9: Potential Energy distribution for spatial single link balancing with a zero free length spring

the link rotates in a horizontal plane, hence, physically there is no meaning for spring balancing against gravity in that case. The fact of the spring constant remaining the same for all other α_1 can be exploited to reduce the computations required for balancing a link with a non-zero-free-length spring connected to the ground by a ball and socket joint. The number of computations decrease drastically as we can reduce the case of a ball and socket joint to a simple single link pivoted to the ground.

This was followed by balancing of the same single spatial link with a spring of non-zero-free-length. In this case α_1 was taken as 45°. The free length of the spring was constrained to lie between 0.075m and 0.15m. For this optimization, we used

$$A = [K \; len]^T \tag{28}$$

The minima obtained was

$$A_{min} = [2483\,\mathrm{N/m}\;0.075\mathrm{m}]^T \tag{29}$$

The peak torque on doing so reduced from 2.77 Nm to 1.17 Nm, i.e. a peak torque reduction of 57.7 %. See Figure 10 for comparison of torque distribution over the entire workspace of the link in balanced and unbalanced state.

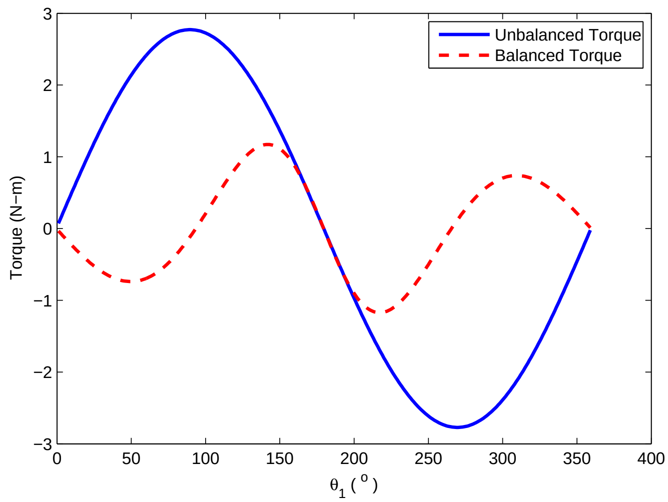

Figure 10: Torque comparison between an unbalanced and balanced spatial link

3.4.2. Spatial two-link balancing

Using potential energy variance minimization, a spatial two link 2-DOF manipulator was balanced. The relevant mechanism parameters arbitrarily chosen were

$$m_2 = 2 \text{ kg},\ m_3 = 2 \text{ kg},$$

$$0.07\text{m} \leq \text{len}_1 \leq 0.08\text{m}, 0.07\text{m} \leq \text{len}_2 \leq 0.08\text{m}$$

$$\alpha_1 = 90°,\ \alpha_2 = 20°,\ \alpha_3 = 45°$$

$$\mathbf{R}_2 = \begin{bmatrix} -0.1 \text{ m} \\ 0 \\ 0 \end{bmatrix}, \mathbf{R}_3 = \begin{bmatrix} -0.1\text{m} \\ 0 \\ 0 \end{bmatrix}$$

$$\mathbf{S}_{12} = \begin{bmatrix} 0 \\ 0 \\ 0.05\text{m} \end{bmatrix}, \mathbf{S}_{21} = \begin{bmatrix} -0.2\text{m} \\ 0 \\ 0 \end{bmatrix}, \mathbf{S}_{23} = \begin{bmatrix} -0.1\text{m} \\ 0 \\ 0 \end{bmatrix}, \mathbf{S}_{32} = \begin{bmatrix} -0.2\text{m} \\ 0 \\ 0 \end{bmatrix}$$

The minima were obtained at

$$A_2 = [715\,\text{N/m}\ 0.07\text{m}]^T, \tag{30}$$

$$A_1 = [7464\,\text{N/m}\ 0.08\text{m}]^T. \tag{31}$$

Table 2 compares the peak torque values for the two links before and after balancing with the designed springs and Figure 11 shows the torque distribution of each link over the configuration space.

The small reduction in peak torque for actuator 2 happens as the link approaches a point of singularity in the workspace. At a singularity the force applied by the spring is unable to generate any torque about the actuator rendering the spring useless resulting in the value of torque to be the same as that of an unbalanced case at the singularity. The effectiveness of spring balancing therefore depends on the workspace of the mechanism as well.

Table 2: Two link spatial manipulator results

Actuator	Unbalanced	Balanced	Torque reduction
	torque (Nm)	torque (Nm)	Optimization
Actuator 1 (proximal)	13.72	3.48	74.6%
Actuator 2 (distal)	3.92	3.59	8.4%

4. Design examples using approximate spring balancing

In this section, the PE variance minimization method is used to design for gravity balancing of a lower-limb orthosis (example of an open kinematic chain) and a manually-operated sit-to-stand wheelchair mechanism (closed kinematic chain). In both cases, the human acts as the actuator.

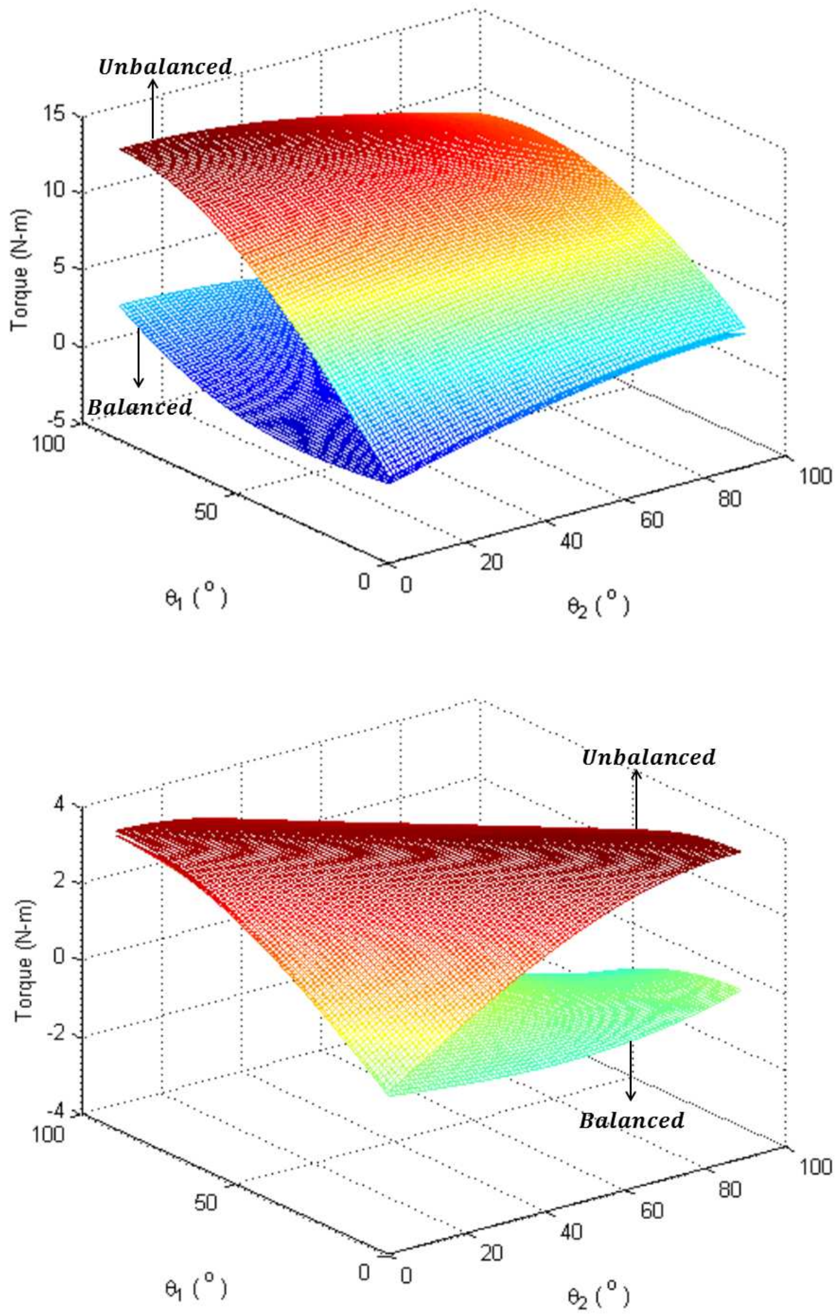

Figure 11: Comparison of unbalanced and balanced torque distribution for actuator 1 (top) and actuator 2 (bottom) over the entire workspace

4.1. Approximate balancing of a two-link lower-limb orthosis

A lower-limb orthosis is a supportive device to enable users with weakened leg muscles (due to various pathologies such as post-polio, spinal cord injury, cerebral palsy, etc.) to walk. Gravity balancing is of tremendous importance for this application since users typically have limited muscular capabilities and the device adds additional weight. [3] present a design for a lower-limb orthosis using static balancing with springs and auxiliary links. We redesign the orthosis with the new method in this section. The movable (with respect to a stationary pelvis) links considered are the femoral and tibial links, so $n = 2$. The relevant values for the various parameters were taken from [3]. The parameters used are:

$$r_2 = 0.177 \text{ m}, r_3 = 0.185 \text{ m}, l_2 = 0.432 \text{ m},$$
$$\alpha_2 = 0°, \alpha_3 = 0°, \beta_{21} = 0°, \beta_{12} = 90°, \beta_{23} = 0°, \beta_{32} = 0°,$$
$$m_2 = 7.39 \text{ kg}, m_3 = 4.08 \text{ kg}, g = 9.8 \text{ m/s}^2,$$
$$240° \leq \theta_2 \leq 300°, \text{ and } (\theta_2 - 60°) \leq \theta_3 \leq \theta_2$$

The range of motion of the links corresponds to normal human walking. The attachment points of the springs were also selected as a part of the control variables for optimal placement of the springs. The constraints placed on this optimization were:

1. Maximum length of the spring should be less than 1.5 times its free length to make sure that the spring is within its feasible range of operation.
2. Minimum length of the spring should be greater than the free length of the spring to ensure that a tension spring is obtained.
3. Spring constant should be greater than 0 and less than 10000 N/m.

The potential energy variance(PE^2_{A2}) is minimized subject to the constraints specified above to obtain A_2:

$$A_2 = \begin{bmatrix} K_2 \\ len_2 \\ \|\mathbf{S}_{23}\| \\ \|\mathbf{S}_{32}\| \end{bmatrix} = \begin{bmatrix} 1128 \text{ N/m} \\ 0.18 \text{ m} \\ 0.26 \text{ m} \\ 0.1 \text{ m} \end{bmatrix}$$

Using A_2, the PE variance(PE^1_{A1}) is minimized subject to the constraints to obtain A_1 as:

$$A_1 = \begin{bmatrix} K_1 \\ len_1 \\ \|\mathbf{S}_{12}\| \\ \|\mathbf{S}_{21}\| \end{bmatrix} = \begin{bmatrix} 2000 \text{ N/m} \\ 0.31 \text{ m} \\ 0.19 \text{ m} \\ 0.26 \text{ m} \end{bmatrix}$$

Gradient-based methods (Active Set, SQP(Sequential Quadratic Programming)) failed to give a global convergence; hence a genetic algorithm was used for this optimization using the MATLAB® optimization toolbox *ga*.

Table 3 shows the torques obtained using minimization of the PE variance and compares the reduction to the values reported in [3]. The torque reduction by the proposed method is lower than the torque reduction by the method used in [3], but the PE variance minimization technique eliminates the need for auxiliary links making the entire mechanism compact and more practical. More parameters such as β's of the spring pivot positions can also be varied. See Figures 12 and 13 for torque variation with (θ_2, θ_3) before and after spring

Table 3: Comparison of results

Actuator	Unbalanced	Balanced	Torque reduction	
	torque (Nm)	torque (Nm)	Optimization	From [3]
1 (Hip Joint)	22.24	6.44	71.0%	90%
2 (Knee Joint)	7.41	3.70	50.0%	50%

balancing. Actual springs were designed for spring 1 and 2 using [20]. The

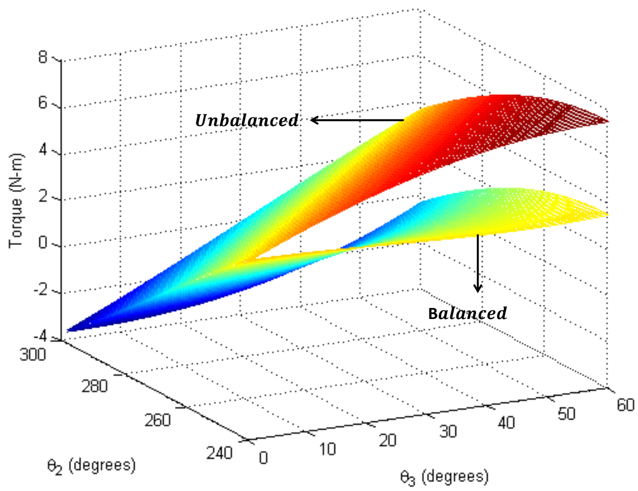

Figure 12: Torque for actuator 2 (knee joint) before and after spring balancing

extension springs so obtained are made of music wire, a commonly used material for springs, and are neither too bulky nor too heavy. Table 4 presents the parameters of the spring design for the two springs used in the orthosis. A

Table 4: Spring design for lower-limb orthosis

Spring	Spring constant (N/m)	Wire diameter (mm)	Coil diameter (mm)	Number of turns	Mass (kg)
1	2000	4	26	76	0.600
2	1128	3	23	60	0.238

schematic of the lower body orthosis was modeled (Figure 14) to visualize the practical space requirement of the designed springs. Note that the direct use of zero-free-length-springs and the absence of auxiliary links and systems to simulate non-zero-free-length springs make this design less complex and more cost-effective.

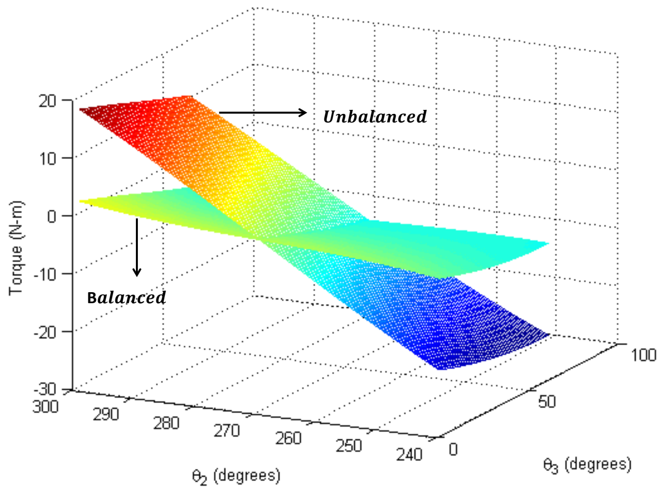

Figure 13: Torque for actuator 1 (hip joint) before and after spring balancing

4.2. Example: Balancing of a sit-to-stand wheelchair

Reducing actuator loads is also important for applications in which human effort is required for actuation. A manually-powered sit-to-stand wheelchair developed in the Rehabilitation Research and Device Development (R2D2) Lab in IIT Madras uses a four-bar mechanism actuated by the user through a driver dyad [21]. Actuator torque minimization is critical since the user has to lift himself/herself from the sitting to the standing position using his/her upper body strength. Balancing by the potential energy variance minimization method for a four-bar linkage was applied to this design problem. The mechanism accomplishing the sit-to-stand motion of the wheelchair is a paralleogram linkage (a-b-c-d) as shown in Figure 15. Note that this parallelogram is not an auxiliary linkage added for balancing. An extension spring was designed to be connected between a-c to utilize the unused space below the seat. The PE for the four-bar

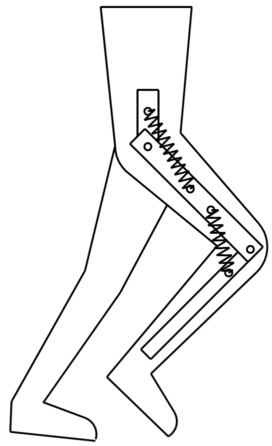

Figure 14: A schematic of the orthosis with the designed springs, modeled to scale

parallelogram linkage is given by

$$\begin{aligned} PE &= m_2 g r_2 \sin(\theta_2 + \alpha_2) + m_3 g(l_2 \sin\theta_2 + r_3 \sin(\theta_3 + \alpha_3)) \\ &\quad + m_4 g(l_1 \sin\theta_1 + r_4 \sin(\theta_4 + \alpha_4)) + \frac{1}{2} K_1(\|\mathbf{S}_{13} - \mathbf{S}_{31} - \mathbf{L}_2\| - len_1)^2 \end{aligned} \tag{32}$$

The configuration space for this application is $0° \leq \theta_2 \leq 85°$. The sit-to-stand device is designed for a person weighing 100 kg. The relevant parameters for the design are taken from [21]:

$$\begin{gathered} m_2 = 103 \text{ kg},\ m_3 = 1.5 \text{ kg},\ m_4 = 3 \text{ kg} \\ l_1 = 200 \text{ mm},\ l_2 = 440 \text{ mm},\ l_3 = 200 \text{ mm},\ l_4 = 440 \text{ mm} \\ r_2 = 220 \text{ mm},\ r_3 = 100 \text{ mm},\ r_4 = 220 \text{ mm}, \\ g = 9.8\ m/s^2,\ \theta_1 = 315°. \end{gathered}$$

The control variables are $A = \begin{bmatrix} len1 \\ K_1 \end{bmatrix}$. Apart from the compulsory constraint on K_1 to ensure that the spring is always in tension, the free length must be less than the minimum length of the spring during operation. $len1 \leq min(\|\mathbf{S}_{13} - \mathbf{S}_{31}\|) = 0.3642$ m and $len_1 \geq 0.1$ m.

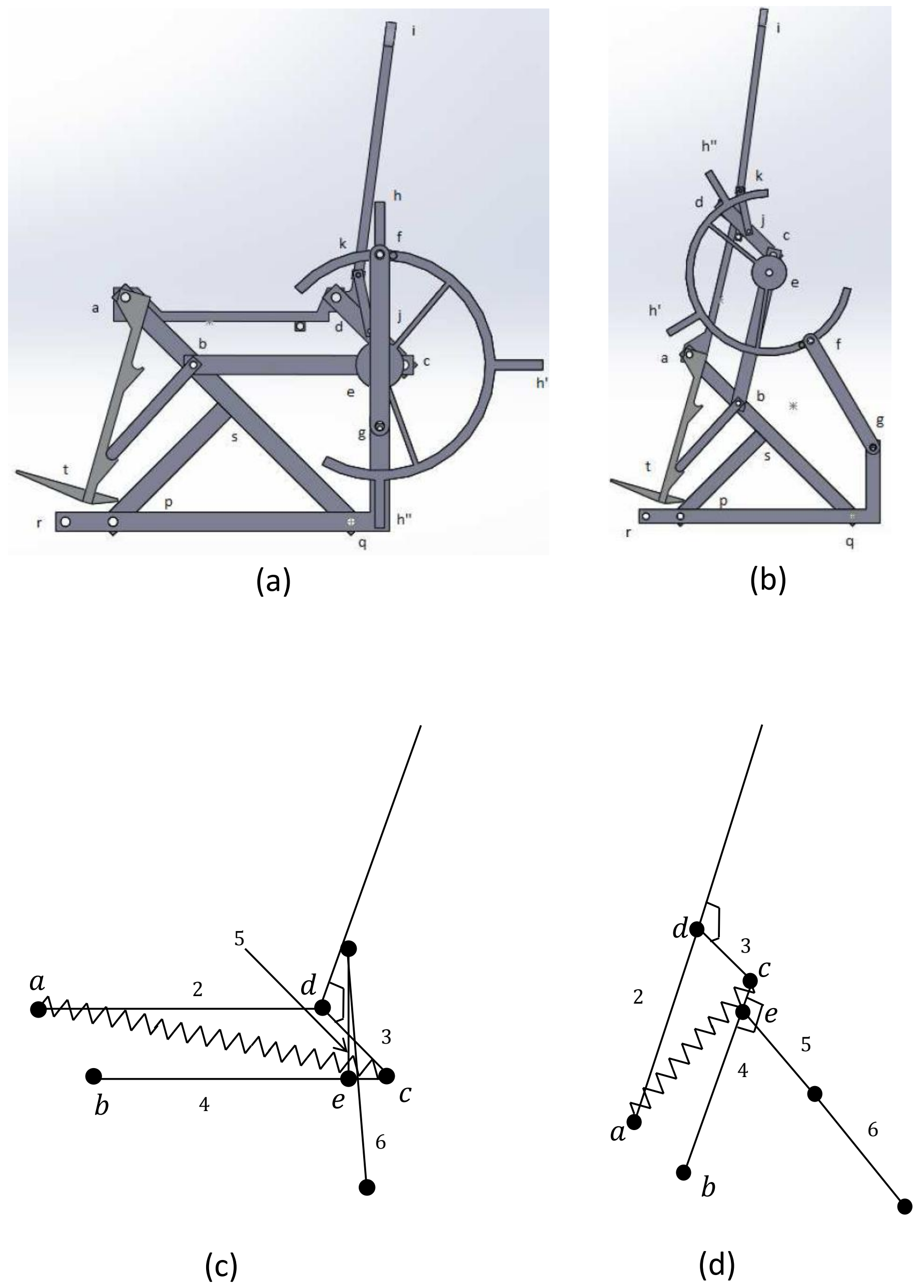

Figure 15: Mechanism of sit-to-stand wheelchair(adapted from [21]).(a) CAD model - sitting position, (b) CAD model - standing position, (c) Kinematic diagram - sitting position, (d) Kinematic diagram - standing position

Minimizing variance(PE_A) subject to the specified constraints results in

$$A = \begin{bmatrix} 0.364 \text{ m} \\ 6902 \text{ N/m} \end{bmatrix}.$$

Since the parallelogram is actuated by a dyad and the user's center of gravity varies as the wheelchair moves from the sitting to the standing position, the force analysis was done using ADAMS®. Figure 16 shows the torque requirement without and with balancing. This is the torque the user has to apply at joint e to lift himself/herself from sitting to the standing position (see Figure 15).

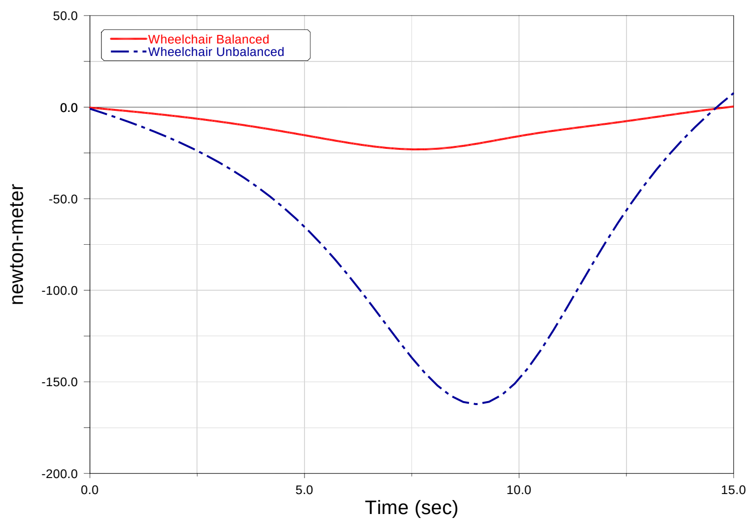

Figure 16: Comparison of wheelchair actuation torque before balancing and after balancing

The torque required to actuate the linkage before and after spring balancing are compared in Table 5. The results obtained after optimization were used to

Table 5: Comparison of results for wheelchair before and after balancing

Torque before balancing (Nm)	Torque after balancing (Nm)	Torque reduction
160	23	85.62%

design a spring using [20]. There are two mechanisms, one on either side of the wheelchair and hence two springs are required. Therefore, the spring constant for the spring design is taken as half of the value obtained by optimization. The material used is music wire and the parameters of the spring designed are specified in Table 6.

Table 6: Spring design for sit-to-stand wheelchair

Spring Constant	Wire Diameter	Coil Diameter	No. of Turns	Mass
3451 N/m	6 mm	40 mm	61.5	1.65 kg

5. Conclusions

This paper presents a new method for static balancing of mechanisms with conservative loads such as gravity and spring loads using non-zero-free-length springs with child-parent connections and no auxiliary links. The method, which involves minimizing the variance of the potential energy, provides substantial reduction in actuator requirements under space constraints. Although the method provides only for approximate balancing, it is versatile, flexible and easy to implement. The true potential of this technique lies in the fact that it uses a very simple optimization to find the spring constant, free-length of the spring and also the optimal attachment points subject to the optimization constraints. Its simplicity and effectiveness would make it a handy tool for designers. The method uses physically realizable non-zero-free-length springs directly, thereby reducing the complexity involved in simulating zero-free-length springs from non-zero-free-length springs. In addition, because auxiliary linkages can be avoided, the resultant mechanisms can be more compact. The cost benefits and reduced complexity can be significant advantages especially in the development of user-actuated rehabilitation devices for developing countries.

Although parallel manipulators have not been dealt with in this paper, the authors believe that this approach of flattening the potential energy distribution over the workspace can be extended to this class of mechanisms as well. Unlike serial manipulators, a sequential optimization may not be possible for parallel manipulators having higher degrees of freedom as the external loads are shared by all actuators. This could potentially complicate the optimization problem.

This method has certain drawbacks as well. The optimal solution for the spring design obtained is dependent on the target workspace of the mechanism as different workspaces have different potential energy distributions. If the workspace contain singularities, i.e. orientations where the spring is unable to generate any torque about the joints, then spring balancing will have no torque reduction for those orientations. Such points should be avoided. Future work will look into avoiding singularities by appropriate placement of springs. Also, as the size of the mechanism and the number of springs in it grow, the time taken for the optimization to converge to a solution increases.

The method based on potential energy is easier to formulate than methods that minimize torque obtained by Eulerian equations. The method provides flexibility in choosing appropriate control variables that are relevant to a particular design problem. However, as with all optimization problems, convergence may be local and may not give the best solution, especially when several control variables are involved.

This paper presents the formulation for planar and spatial open kinematic chains, for a planar four-bar linkage, and illustrates application to a lower-limb orthosis and a sit-to-stand wheelchair. Design of a prototype of the orthosis and incorporation of spring balancing in the wheelchair prototype are currently in progress. The method of approximate spring balancing using minimization of the potential energy variance can be extended to balancing using torsional springs, and can find wide application in the area of robotics, as well.

6. Nomenclature

$\mathbf{S}_{ij}$ - The position vector of the attachment point of spring connecting body i and body j on body i, measured from the parent pivot of body i.

$\mathbf{R}_i$ - The position vector of the centre of mass of the ith link from the parent pivot of the ith body.

$\mathbf{L}_i$ - The position vector from joint $i-1$ to joint i for all $i > 2$

r_i - $\|\mathbf{R}_i\|$

l_i - Kinematic length of the ith link

β_{ij} - Angle of $\mathbf{S}_{ij}$ with respect to the kinematic line of the ith link measured counterclockwise (β_{12} is the only exception measured from horizontal)

α_i - Angle of $\mathbf{R}_i$ with respect to the kinematic line of the ith link measured counterclockwise

θ_i - Angle of the kinematic line of the ith link measured counterclockwise from horizontal (Assumed 0 for ground)

m_i - Mass of the ith link

K_i - Spring constant of the spring connecting body i and i+1

len_i - Free length of the spring connecting body i and i+1

g - acceleration due to gravity (9.8 m/s^2)

PE - Total Potential Energy

References

[1] T. Rahman, R. Ramanathan, R. Seliktar, and W. Harwin. A simple technique to passively gravity-balance articulated mechanisms. *Journal of Mechanical Design*, 117(4):655–658, 1995.

[2] D.A. Streit and E. Shin. Equilibrators for planar linkages. *Journal of Mechanical Design*, 115(3):604–611, 1993.

[3] A. Agrawal and S. K. Agrawal. Design of gravity balancing leg orthosis using non-zero free length springs. *Mechanism and Machine Theory*, 40(6):693–709, June 2005.

[4] A. Gopalswamy, P. Gupta, and M. Vidyasagar. A new parallelogram linkage configuration for gravity compensation using torsional springs. In *Proceedings of IEEE International Conference on Robotics and Automation*, pages 664–669, Nice, France, May 1992.

[5] G Carwardine. Improvements in elastic force mechanisms. *UK Patent*, 377, 1932.

[6] F.L.S. te Riele and J.L. Herder. Perfect static balance with normal springs. In *Proceedings of the ASME Design Engineering Technical Conference*, pages 9–12, Pittsburg, Pennsylvania, September 2001.

[7] S.R. Deepak and G.K. Ananthasuresh. Perfect static balance of linkages by addition of springs but not auxiliary bodies. *Journal of Mechanisms and Robotics*, 4(2):021014, 2012.

[8] S. Segla, C.M. Kalker-Kalkman, and A.L. Schwab. Statical balancing of a robot mechanism with the aid of a genetic algorithm. *Mechanism and Machine Theory*, 33(1):163 – 174, 1998.

[9] C. Huang and B. Roth. Dimensional synthesis of closed-loop linkages to match force and position specifications. *Journal of Mechanical Design*, 115(2):194–198, 1993.

[10] C. Huang and B. Roth. Position-force synthesis of closed-loop linkages. *Journal of Mechanical Design*, 116(1):155–162, 1994.

[11] S. Mahalingam and A. Sharan. The optimal balancing of the robotic ma-

nipulators. In *Proceedings of IEEE International Conference on Robotics and Automation*, San Francisco, CA USA, April 1986.

[12] S. Idlani, D. A. Streit, and B. J. Gilmore. Elastic potential synthesis—a generalized procedure for dynamic synthesis of machine and mechanism systems. *Journal of Mechanical Design*, 115(3):568–575, 1993.

[13] M.L. Brinkman and J.L. Herder. Optimizing a balanced spring mechanism. In *Proceedings of the ASME Design Engineering Technical Conference*, Montreal, Canada, September 2002.

[14] S. K. Agrawal and A. Fattah. Theory and design of an orthotic device for full or partial gravity-balancing of a human leg during motion. *IEEE Transactions On Neural Systems and Rehabilitation Engineering*, 12(2):157–165, June 2004.

[15] S. K. Banala, S. K. Agrawal, A. Fattah, V. Krishnamoorthy, W. L. Hsu, J. Scholz, and K. Rudolph. Gravity-balancing leg orthosis and its performance evaluation. *IEEE Transactions On Robotics*, 22(6):1228–1239, December 2006.

[16] T. Nakayama, Y. Araki, and H. Fujimoto. A new gravity compensation mechanism for lower limb rehabilitation. In *Proceeedings of International Conference on Mechatronics and Automation*, pages 943–948, Changchun, China, August 2009. IEEE.

[17] L. Ciupitu, I. Simionescu, and A. Olaru. Static balancing of mechanical systems used in medical engineering field–continuous balancing. *Advanced Materials Research*, 463:890–894, 2012.

[18] M.W. Spong and M. Vidyasagar. *Robot Dynamics and Control*. John Wiley & Sons, New York, 2008.

[19] M.W. Spong, S. Hutchinson, and M. Vidyasagar. *Robot Modeling and Control*. John Wiley & Sons, New York, 2006.

[20] R.L. Norton. *Machine Design: An Integrated Approach*. Prentice-Hall, New York, 1996.

[21] H. Chaudhari. Design of a standing wheelchair. Dual degree project report, IIT Madras, 2012.

List of Figures